Surface temperature measurement through surface plasmon resonance

Joyce Ibrahim, Mostafa Al Masri, Isabelle Verrier, Colette Veillas, Frédéric Celle, Serge Cioulachtjian, Olivier Parriaux, Frédéric Lefèvre, Yves Jourlin

Temperature sensor through surface plasmon resonance

Joyce Ibrahim[a], Mostafa Al Masri[b], Isabelle Verrier*[a], Colette Veillas[a], Frédéric Celle[a], Serge Cioulachtjian[b], Olivier Parriaux[a], Frédéric Lefèvre[b], Yves Jourlin[a]
[a]Univ. Lyon, UJM-Saint-Etienne, CNRS, Institut d'Optique Graduate School, Laboratoire Hubert Curien, UMR CNRS 5516, 42000 Saint-Etienne, France
[b]Centre de Thermique de Lyon, UMR 5008 CNRS INSA Univ. Lyon, INSA-Lyon, F-69621 Villeurbanne, France

Abstract

The aim of this work is to highlight the possibility of local non-intrusive temperature measurements at the interface between a metallic surface and a fluid by analyzing the plasmon resonance on a periodically micro-structured surface. A change in the temperature of the sample surface induces a modification of the local refractive index leading to a shift of the surface plasmon resonance frequency due to interactions between the evanescent electric field and the close environment of the surface. The metallic gratings developed in this study enable a direct excitation of a plasmonic wave, which, in turn, lead to a high sensibility of the local temperature measurement with a very compact and simple device.

Keywords: Plasmon resonance, temperature sensor, diffraction grating

1. INTRODUCTION

Measurement of the local temperature at the interface between a solid and a liquid is a challenging issue, especially in liquid-vapor equilibrium conditions[1]. Indeed, Infrared thermography measurements are not possible through a liquid and any local measurements using a contact probe would interfere with the experiment and affect the results. As a result, the solid-liquid interface temperature cannot be measured directly but needs to be estimated using a remote probe associated with an inverse approach. The plasmonic sensor is a tool of choice for such an application since it can detect any change in the environment around the surface where the plasmon propagates[2-5]. This type of sensor is already widely used for biological or environmental applications[6-8] but little for thermal applications.

In this work, we present a test rig using the plasmonic resonance to measure the local temperature of an aluminum sample surrounded by acetone in liquid-vapour equilibrium conditions. The sample is enclosed in a chamber where pressure is controlled. A diffraction grating on the surface of the sample makes it possible to couple the light beam located outside the chamber to the plasmonic wave. This measurement method has already been used for the detection of acetone condensation on the surface of the diffraction grating[9]. A shift in the plasmonic wavelength resonance was measured when acetone condensation on the aluminum surface takes place due to a change of the surrounding medium close to the surface. Indeed, the position of the resonance wavelength and its amplitude depend on the characteristics of the diffraction grating (material, period, depth) and of the surrounding medium (permittivity, incidence angle of the wave in this medium). Thus, in the same way, as the temperature of the surrounding medium increases, its permittivity decreases and induces a shift of the resonance towards smaller wavelengths. This method is therefore applied here to the measurement of the temperature of the surface.

First, the parameters of the diffraction grating are chosen so as to obtain a plasmon resonance of optimum amplitude and width at room temperature and the resonance peak is studied as a function of temperature. Then, the complete device with the controlled pressure and temperature chamber is presented as well as the experimental results, which are finally discussed and compared to the theoretical predictions.

*isabelle.verrier@univ-st-etienne.fr

2. MODELIZATION OF THE DIFFRACTIVE GRATING

Simulations have been made in order to maximize the surface plasmon resonance (SPR) and to estimate its evolution for increasing temperature. The optical signal depends on the period, the depth, the profile and the material of the grating, as well as on the properties of the surrounding medium and on the polarization, the angle and the wavelength of the incident light: it reaches maximum amplitude of absorption (dip in the 0^{th} reflected order) for Transverse Magnetic (TM) polarized incident light absorption on 1D grating structures[10-12].

The chosen material is aluminum, which has both suitable plasmonic[13] and thermal characteristics. The 1D structure is shown in Figure 1(a). The resist grating profile, coated by a thin layer of aluminum, is sinusoidal in order to obtain the best plasmonic signature. The substrate is aluminum and the surrounding medium is acetone, which refractive index is around n = 1.36 at room temperature.

2.1 Grating design

Simulations enable to optimize parameters such as incident angle of light θ, period Λ and depth d of the grating and the aluminum thickness e for the best plasmonic resonance for a given wavelength (figure 1(a)). The optical behavior of 1D gratings at room temperature in acetone was modeled using a commercial program (MC grating) that is based on Chandezon method[14-15].

Figure 1(b) shows the reflectance curves for two wavelengths Λ = 760 nm and Λ = 1000 nm with an aluminum layer thickness e = 50 nm, a grating depth d = 55 nm and an incidence angle in acetone θ = 25°. The plasmonic resonance occurs at wavelength around λ_R = 600 nm for the period Λ = 760 nm and around λ_R = 780 nm for the period Λ = 1000 nm. The period is chosen to be Λ = 760 nm in order to have the resonance near the middle of the visible range. Keeping the period Λ = 760 nm, with the aluminum layer thickness e = 50 nm, a grating depth d = 55 nm, the incidence angle is now scanned from θ = 23° to θ = 38°. The value θ = 25° enables to have a narrow resonance in the desired spectral range (Figure 1(c)). A grating depth d = 55 nm (Figure 1(d)) leads to a high resonance amplitude (for Λ = 760 nm, e = 50 nm and θ = 25°). It has to be noticed that the aluminum layer thickness is chosen to be e > 40 nm so that no part of the incident signal is transmitted into the photoresist and the aluminum layer is seen as infinite.

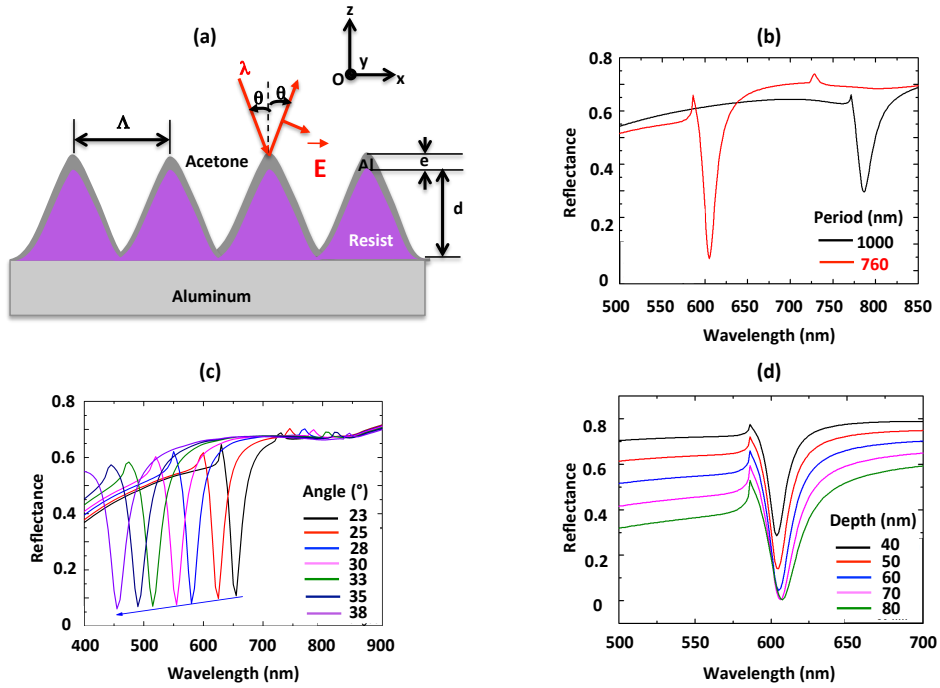

Figure 1. 1D grating in acetone: (a) Scheme of the structure, simulation of the reflectance in TM polarization for: (b) periods Λ = 760 nm and Λ = 1000 nm (aluminum layer thickness e = 50 nm, grating depth d = 55 nm and incidence angle θ = 25°), (c) different incidence angles (Λ = 760 nm, e = 50 nm and d = 55 nm), (d) different grating depths (Λ = 760 nm, e = 50 nm and θ = 25°).

According to this study, a sinusoidal grating has been designed for an optimized resonance, leading to the following grating parameters: period Λ = 760 nm, depth d = 55 nm, aluminum thickness e = 50 nm (> 40 nm). Incidence angle in acetone is θ = 25° corresponding to an incident angle in air θ_{air} = 32° outside the two-phase chamber filled with acetone and containing the grating.

2.2 Theoretical wavelength resonance versus temperature

In order to understand the behavior of the plasmon resonance as function of the temperature, simulations were carried out to investigate the change of the refractive index of acetone with the temperature (the simulations of Figure 1 subsection 2.1 were done at room temperature). Indeed, the refractive index of acetone is decreasing with temperature as shown in Figure 2(a). At wavelength λ_D = 589 nm, the experimental refractive index values were obtained using a temperature controlled Abbe refractometer in the range 22°C – 43°C and theoretical values from the formula[16]:

$$n_D(T°) = n_{D20°} - 0.00045(T°-20) \qquad \text{with } n_{D20} = 1.3595 \tag{1}$$

There is a slight difference in the slope between the experimental and the theoretical values of the acetone refractive index as a function of temperature. This is possibly due to impurities in the acetone. The simulation of the zero order spectra was done from the extrapolated curve of the measured values of acetone refractive index, detecting the corresponding resonance wavelength for each temperature (Figure 2(b)). The change of aluminum permittivity and of the refractive angle in acetone (keeping θ_{air} = 32°) as a function of temperature were also taken into account.

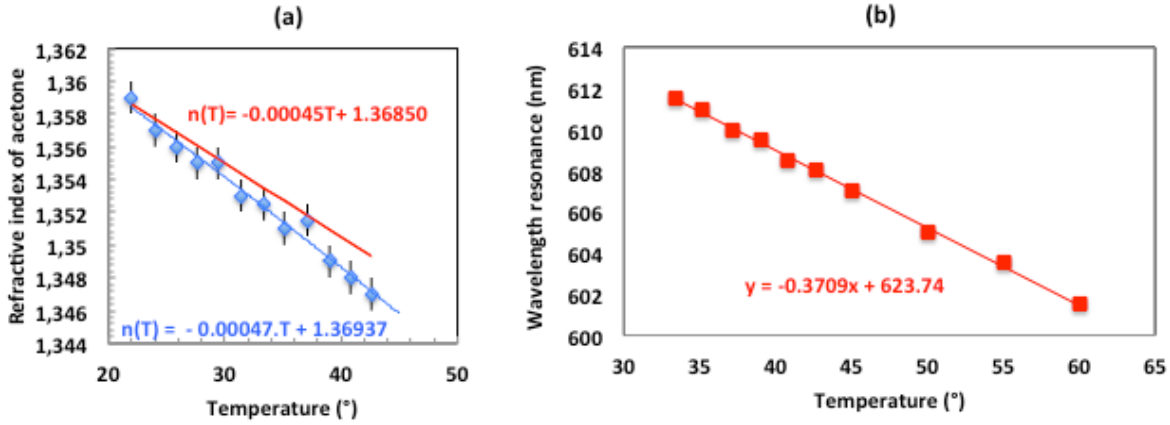

Figure 2. (a) Refractive index of acetone and (b) theoretical resonance wavelength versus temperature.

The theoretical plasmon resonance wavelength (Figure 2(b)) thus varies linearly as a function of temperature in the range 34° < T < 60° with a slope of $\Delta\lambda_R/\Delta T$ = 0.3709 nm/K. These theoretical results are verified experimentally in paragraph 5 where the optical measurement results are presented in details.

3. FABRICATION OF THE GRATING

The gratings were fabricated using a nanoimprint process[17] developed by SILSEF Company. Beforehand, the nanoimprint master fabrication was done in the Hubert Curien laboratory via laser interference lithography (Figure 3 (a)), resulting in a sinus profile grating whose parameters are conform to the simulation. A PDMS mold was then copied from the master diffraction grating and used for the nanoimprint process (Figure 3 (b)). Grating fabrication was finally followed by the deposition of 50 nm of aluminum by sputtering (Figure 3 (c)). This imprinted layer is thick enough to neglect the optical effect of the resist structure underneath.

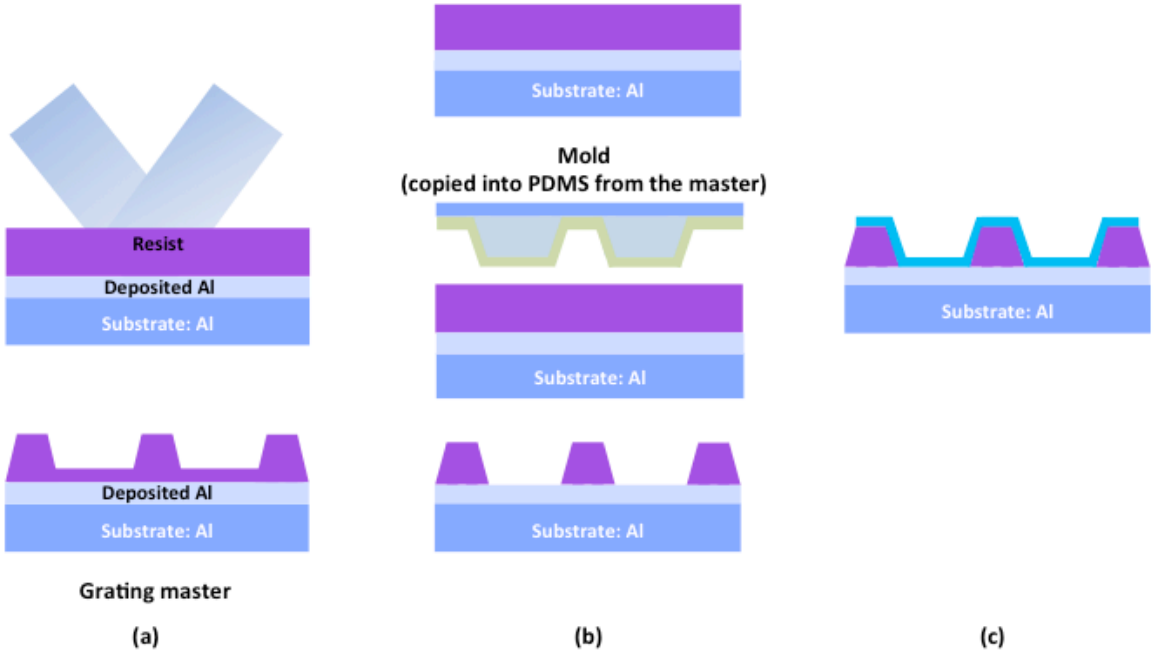

Figure 3. Fabrication process of the grating: (a) Master fabrication, (b) Nanoimprint process, (c) Aluminum deposition.

Figure 4(a) shows the photograph of the 1D grating nanostructure after nanoimprint and aluminum deposition. The image obtained by Atomic Force Microscopy (AFM) shows a quasi-sinusoidal profile, with a period Λ = 760 nm and a depth d = 55 nm of the grating close enough to the desired optimized structure (Figure 4(b) and 4(c)).

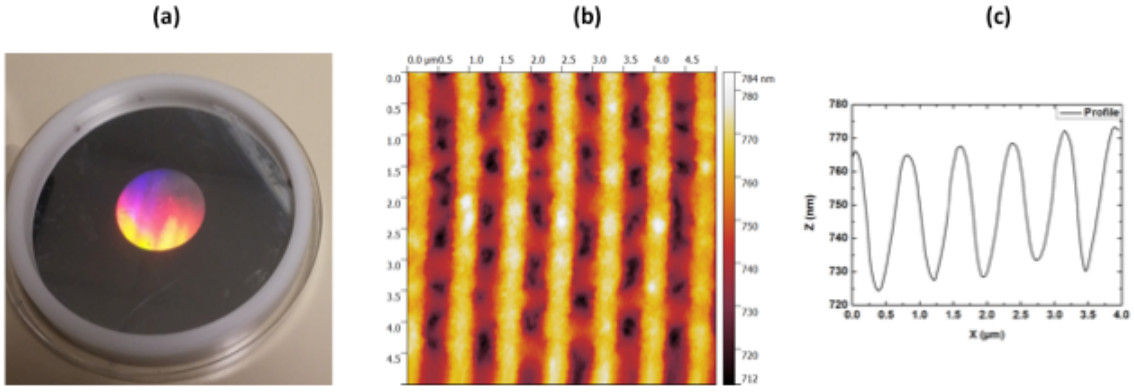

Figure 4. Grating: (a) Photograph, (b) 2D AFM image, (c) AFM profile.

In the following paragraph, this grating structure has been used in the reflectance measurement set-up as a sensor to detect a temperature change at the metallic surface.

4. EXPERIMENTAL BENCH

The grating was set up vertically in a hermetically sealed reservoir filled with liquid acetone at constant pressure and controlled temperature. Acetone was heated by a hotplate located behind the reservoir. Temperature is controlled by two thermocouples inserted inside the chamber. The experimental bench for measuring the plasmonic resonance and consequently the surface temperature of the grating immersed in acetone is shown in the Figure 5. A collimated and enlarged beam issued from a fiber connected to a halogen source illuminates the grating on a surface of approximately 50 mm^2 with an incidence angle of θ_{air} = 32° through the transparent window of the chamber. The polarizer is oriented in such manner that the beam is TM polarized. The reflected beam is focalized into an optical fiber connected to a spectrometer and analyzed by the spectrometer software.

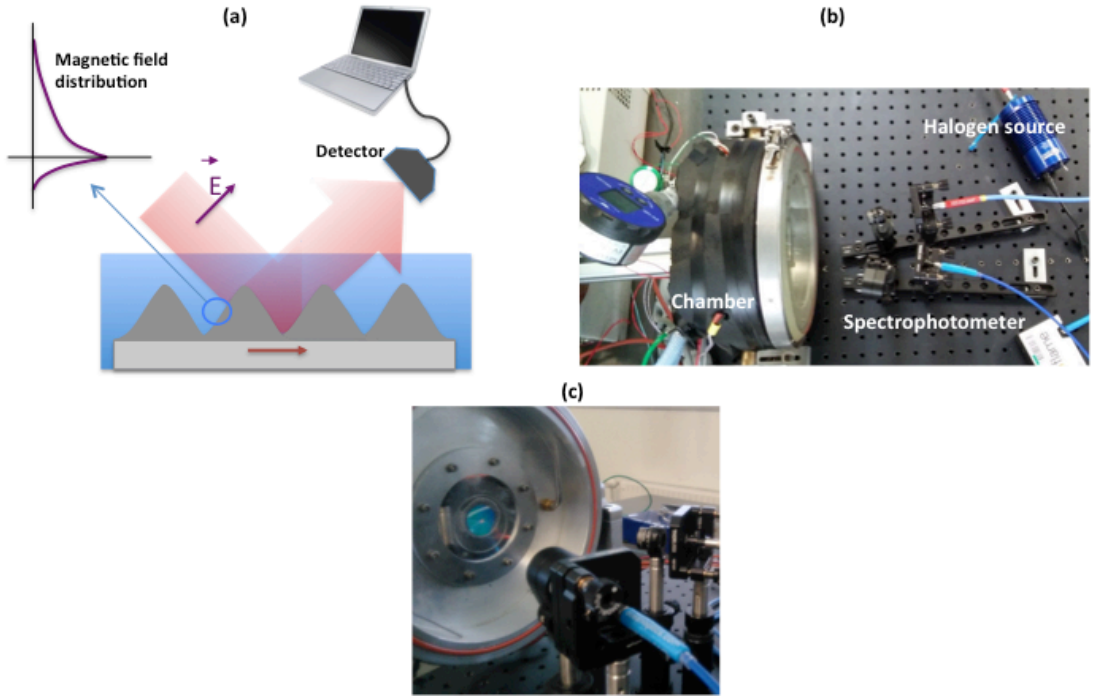

Figure 5. Temperature sensor bench: (a) Set-up scheme, (b) top view photograph, (c) front view photograph.

5. RESULTS AND DISCUSSION

Figure 6 presents preliminary results obtained to verify the shift in the plasmon resonance wavelength for increasing acetone temperature in the measurement range 34 °C < T < 60 °C. The chamber was initially maintained at T_0 = 34 °C. The plasmon resonance was measured from the record wavelength spectrum measured for several increasing temperatures (Figure 6(a)). Measurements were performed in the center of the sample and normalized with respect to the reflectance of the unstructured aluminum on the same sample. The maximum absorption position of each reflectance curve, which corresponds to the plasmonic resonance wavelength, shifts to smaller wavelengths as the temperature increases, from λ_R = 603 nm (T_0 = 34° C) to λ_R = 594 nm (T = 60 °C). The experimental data were fitted by a linear function of the temperature, resulting in a slope of $\Delta\lambda_R/\Delta T$ = 0.3806 nm/K.

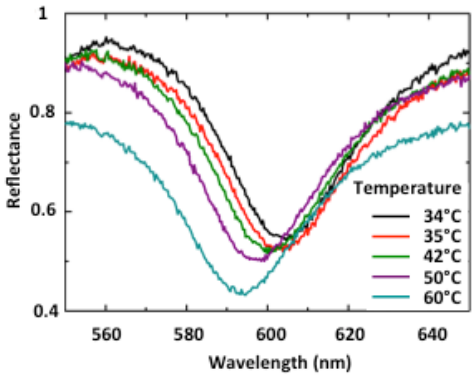

Figure 6. Experimental wavelength spectra as a function of temperature.

Then, further measurements at higher temperatures 54 °C < T <150 °C were performed with a more precise estimation of the experimental resonance wavelengths by adjusting each spectrum with a Gaussian function and by interpolating the value of the minimum (Figure 7).

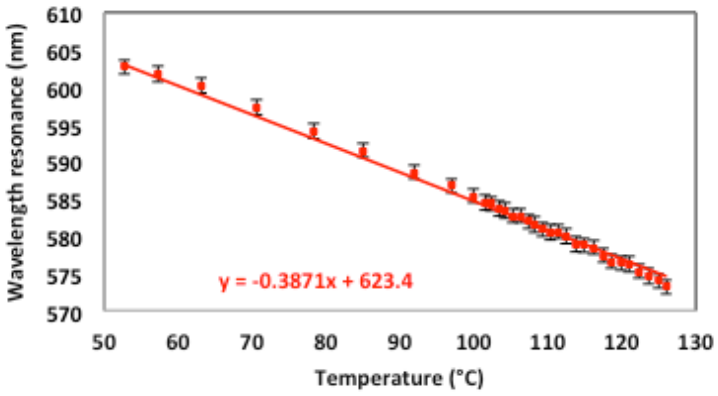

Figure 7. Resonance wavelengths as a function of temperature.

The sensitivity of the sensor $\Delta\lambda_R/\Delta T$ = 0.3871 nm/K is almost the same as for the lowest temperatures and matches well to the predicted one (0.3709 nm/K in Figure 2(b)) within the measurement uncertainties.

The absolute value of the measured resonance wavelengths is slightly smaller than theoretically expected. This may be due to an error in the experimental incidence angle that could be not accurately enough adjusted. Indeed a shift of 0.5° of $\Delta\theta_{air}$ induces theoretically an offset of $\Delta\lambda$ = 8 nm.

The minimum of temperature variation that could be measured is linked to the sensitivity of the spectrometer and to the valuation method of the minimum resonance wavelength. The uncertainty due to the resolution of the spectrometer leads to a value of $\Delta\lambda_R$ = 0.28 nm inducing a minimum detectable variation of the temperature of ΔT = 1.3 K. However, if we change the slit of the spectrometer, the uncertainty related to its resolution can be reduced by a factor of 10.

The experimental set-up demonstrated that SPR can be used as a non-invasive temperature measurement method of a metallic surface with 1°C resolution over a temperature range from 34°C to 125°C. But, with better spectroscopic equipment, an improvement of the resolution to an uncertainty of 0.1K can be expected.

6. CONCLUSION

In this study, a technique for temperature measurement at an interface between a fluid and a solid surface was presented. A plasmonic submicronic structure was used as a sensor. The structured surface was fabricated by nanoimprint and investigated using AFM characterization showing a sinusoidal 1D grating profile. The reflected spectrum was studied while increasing the temperature in the chamber and the change of the spectral position of the resonance was measured. This technique can be used for real time and non-invasive measurement of the temperature at a surface surrounded by a liquid. The method is very sensitive to refractive index changes and thus well adapted to the temperature change at the surface.

FUNDING

The support from the French National Research Agency (ANR) within the ‘‘NUCLEI’’ project (ANR-12-SEED-0003) is gratefully acknowledged.

ACKNOWLEDGEMENTS

The authors would like to thanks HEF for aluminum deposition and the company SILSEF for the grating fabrication using nanoimprint technique.

REFERENCES

[1] Al Masri, M., Cioulachtjian, S., Veillas, C., Verrier, I., Jourlin, Y., Ibrahim, J., Martin, M., Pupier, C., Lefèvre, F., "Nucleate boiling on ultra-smooth surfaces: explosive incipience and homogeneous density of nucleation sites," Experimental Thermal and Fluid Science **88,** 24-36 (2017).

[2] Maier, S. A., [Plasmonics Fundamentals and Applications], Springer, New York (2007).

[3] Shahbazyan, T. V. and Stockman, M.I., [Plasmonics: theory and applications], Springer, Dordrecht, (2014).

[4] Homola, J., Yee, S. S. and Gauglitz, G., "Surface plasmon resonance sensors: review," Sens. Actuators B Chem. 54(1–2), 3–15 (1999).

[5] Porto, J. A., Garcta-Vidal, F. J. and Pendry, J. B., "Transmission resonances on metallic gratings with very narrow slits," Phys. Rev. Lett. 83(14), 2845–2848 (1999).

[6] Homola, J., "Surface plasmon resonance sensors for detection of chemical and biological species," Chem. Rev. 108(2), 462–493 (2008).

[7] Jiang, S., Peng, Y., Ning, B., Bai, J., Liu, Y., Zhang, N. and Gao, Z., "Surface plasmon resonance sensor based on molecularly imprinted polymer film for detection of histamine," Sens. Actuators B Chem. 221, 15–21 (2015).

[8] Vala, M., Chadt, K., Piliarik, M. and Homola, J., "High-performance compact SPR sensor for multi-analyte sensing," Sens. Actuators B Chem. 148(2), 544–549 (2010).

[9] Ibrahim, J., Al Masri, M., Veillas, C., Celle, F., Cioulachtjian, S., Verrier, I., Lefèvre, F., Parriaux, O. and Jourlin, Y., "Condensation phenomenon detection through surface plasmon resonance," Optics Express, 25 (20), 24189-24198 (2017).

[10] Arriola, A., Rodriguez, A., Perez, N., Tavera, T., Withford, M. J., Fuerbach, A. and Olaizola, S. M., "Fabrication of high quality sub-micron Au gratings over large areas with pulsed laser interference lithography for SPR sensors," Opt. Mater. Express 2(11), 1571–1579 (2012).

[11] Jourlin, Y., Tonchev, S., Tishchenko, A. V., Pedri, C., Veillas, C., Parriaux, O., Last, A. and Lacroute, Y., "Spatially and polarization resolved plasmon mediated transmission through continuous metal films," Opt. Express 17(14), 12155–12166 (2009).

[12] Qu, Y., Li, Q., Gong, H., Du, K., Bai, S., Zhao, D., Ye, H. and Qiu, M., "Spatially and spectrally resolved narrowband optical absorber based on 2D grating nanostructures on metallic films," Adv. Opt. Mat. 4(11), 480–486 (2016).

[13] Knight, M. W., Liu, L., Wang, Y., Brown, L., Mukherjee, S., King, N. S., Everitt, H. O., Nordlander, P. and Halas, N. J., "Aluminum plasmonic nanoantennas," Nano Lett. 12(11), 6000–6004 (2012).

[14] Lyndin, N. M., "MC grating," (2014). http://mcgrating.com.

[15] Jourlin, Y., Tonchev, S., Tishchenko, A. V. and Parriaux, O., "Sharp plasmon-mediated resonant reflection from an undulated metal layer," IEEE photonics Journal **6** (5), (2014).

[16] http://culturesciences.chimie.ens.fr/content/le-refractometre-916.

[17] Boltasseva, A., "Plasmonic components fabrication via nanoimprint," J. Opt. A **11,** 4801906 (2009).